Clinical Cancer Research

MicroRNA-374b Suppresses Proliferation and Promotes Apoptosis in T-cell Lymphoblastic Lymphoma by Repressing AKT1 and Wnt-16

Dong Qian[1,2], Kailin Chen[2,3], Haixia Deng[2], Huilan Rao[2,4], Huiqiang Huang[2,3], Yiji Liao[2], Xiaofei Sun[2,5], Suying Lu[2,5], Zhiyong Yuan[1], Dan Xie[2,4], and Qingqing Cai[2,3]

Abstract

Purpose: Deregulation of microRNA (miRNA) has been extensively investigated in both Hodgkin and non-Hodgkin lymphomas (NHL); however, little is known about the roles of miRNAs in T-cell lymphoblastic lymphoma (T-LBL). The aim of the present study was to investigate the potential roles of miR-374b in the development and treatment of T-LBL.

Experimental Design: MiRCURY LNA array was used to generate a miRNA-expressing profile. Real-time quantitative PCR and immunohistochemistry (IHC) were applied to detect the expression of miR-374b, AKT1, and Wnt16 in T-LBL samples. The dual-luciferase reporter assay was conducted to confirm target associations of miR-374b. The tumor-suppressive effect of miR-374b was determined by both *in vitro* and *in vivo* studies.

Results: The expression of 380 miRNAs was evaluated in five human T-LBL tissues and five infantile thymus samples by microRNA microarrays. Downregulation of miR-374b was frequently detected in primary T-LBL tissues, which was significantly associated with worse overall survival and increased risk of recurrence of the 58 patients enrolled in this study. miR-374b suppressed T-LBL cell proliferation *in vitro* and *in vivo* and sensitized cells to serum starvation- and chemotherapeutic agent-induced apoptosis. Furthermore, we characterized two AKT pathway–associated molecules, AKT1 and Wnt16, as direct targets of miR-374b. Consistently, in T-LBL patient tissues, AKT1 and Wnt16 expression was inversely correlated with miR-374b levels, and was an independent predictor of recurrence and survival.

Conclusions: Our data highlight the molecular etiology and clinical significance of miR-374b in T-LBL. Targeting miR-374b may represent a new therapeutic strategy to improve therapy and survival for T-LBL patients. *Clin Cancer Res; 21(21); 4881–91. ©2015 AACR.*

Downloaded from http://aacrjournals.org/clincancerres/article-pdf/21/21/4881/2027063/4881.pdf by guest on 24 August 2022

Introduction

MicroRNAs (miRNA) belong to a class of phylogenetically conserved noncoding RNAs that suppress protein expression through base pairing with 3′-untranslated regions (3′-UTR) of target genes (1, 2). Emerging evidence suggests that miRNAs are aberrantly expressed during the development and progression of a variety of human cancers, including leukemia and lymphoma (3–5).

Lymphoblastic lymphoma (LBL) is a rare heterogeneous group of immature B cells committed to the B-cell lineage (B-LBL) or T-cell lineage (T-LBL) whose incidence accounts for approximately 1% to 2% of non-Hodgkin lymphomas (NHL) worldwide (6, 7). T-LBL comprises about 90% of all LBL that are typically seen in late childhood, adolescence, and young adulthood with a male predominance (8, 9). T-LBL is a chemotherapy-sensitive disease with a 75% to 85% event-free survival rate using current treatment regiments. However, because of frequent relapse, the 5-year overall survival rate is poor (30%–50%; refs. 10, 11). Furthermore, 5-year survival in relapsed patients is only 10% to 15% (12, 13). Therefore, reliable markers to predict T-LBL relapse and prognosis are highly desired to optimize therapeutic strategies and improve clinical outcomes. Deregulation of miRNAs has been extensively investigated in both Hodgkin lymphoma and NHL (4, 14). Higher levels of miR-155, miR-21, and miR-221 predict a poor prognosis for diffuse large B-cell lymphoma (15–17). Reduced expression of miR-143 and miR-145 has also been documented in B-cell malignancies, and reexpression of these miRNAs in a Burkitt lymphoma cell line demonstrated a dose-dependent growth-inhibitory effect (18). These findings suggest the involvement of miRNAs in the pathogenesis of lymphoma, and miRNAs can be effective biomarkers to predict outcomes and improve therapy responses of patients with lymphoma. Most recently, Mussolin and colleagues have reported the first characterization of childhood T-LBL by miRNA expression

[1]Department of Radiotherapy, Tianjin Medical University Cancer Institute and Hospital, National Clinical Research Center for Cancer, Key Laboratory of Cancer Prevention and Therapy, Tianjin, P.R. China. [2]State Key Laboratory of Oncology in South China, Cancer Center, Sun Yat-Sen University, Collaborative Innovation Center of Cancer Medicine, Guangzhou, P.R. China. [3]Department of Medical Oncology, Cancer Center, Sun Yat-sen University, Guangzhou, P.R. China. [4]Department of Pathology, Cancer Center, Sun Yat-sen University, Guangzhou, P.R. China. [5]Department of Pediatric Oncology, Cancer Center, Sun Yat-sen University, Guangzhou, P.R. China.

Note: Supplementary data for this article are available at Clinical Cancer Research Online (http://clincancerres.aacrjournals.org/).

D. Qian, K. Chen, and H. Deng contributed equally to this article.

Corresponding Authors: Qingqing Cai, Department of Medical Oncology, Cancer Center, Sun Yat-sen University, 651 Dong Feng Road East, Guangzhou 510060, P.R. China. Phone: 86-20-87342562; Fax: 86-20-87342562; E-mail: caiqq@sysucc.org.cn; and Dan Xie, State Key Laboratory of Oncology in South China, Cancer Center, Sun Yat-Sen University, 651, Dong Feng Road East, Guangzhou 510060, P.R. China. Phone: 86-20-87343193; Fax: 86-20-87343170; E-mail: xied@mail.sysu.edu.cn

doi: 10.1158/1078-0432.CCR-14-2947

©2015 American Association for Cancer Research.

Translational Relevance

MicroRNAs are aberrantly expressed during the development and progression of a variety of human cancers, including leukemia and lymphoma; however, little is known about miRNAs in T-LBL. Here, we found that miR-374b was significantly downregulated in the T-LBL tissues by microRNA microarray assays, and the downregulation of miR-374b was significantly associated with a high risk of relapse and worse overall survival in T-LBL patients. Our *in vitro* and *in vivo* studies showed that ectopic restoration of miR-374b suppressed cell proliferation and tumorigenicity and promoted cellular apoptosis by inhibiting the AKT signal pathway through repressing Wnt-16 and AKT1 expression. Furthermore, Wnt-16 and AKT1, two direct targets of miR-374b, could also be independent predictors of patients' survival and relapse. Thus, miR-374b together with downstream factors may be used as novel prognostic biomarkers and promising therapeutic target for patients with T-LBL.

profiling and identified some miRNAs that are deregulated in T-LBL (19). However, little is known about miRNAs in the development and treatment of T-LBL. Therefore, extensive investigations on the functions of miRNAs that are deregulated in T-LBL are required.

In this study, for the first time, we report that the downregulation of miR-374b is significantly associated with the survival of T-LBL patients. Moreover, *in vitro* and *in vivo* studies demonstrate that ectopic restoration of miR-374b promotes apoptosis and suppresses proliferation T-NHL cells through repressing the AKT signaling pathway. Our findings highlight the functions and roles of miRNAs in T-LBL, and suggest miR-374b could be used as a novel prognostic marker and potential therapeutic target for T-LBL patients.

Materials and Methods

Tissue specimens and cell cultures

T-LBL tissue samples were obtained with informed consent under Institutional Review Board–approved protocols. The samples were collected at the Cancer Center, Sun Yat-Sen University (Guangzhou, China). The T-LBL cases selected were based on clear pathologic diagnosis and follow-up data, and were from patients that had not received previous local or systemic treatment. The infantile thymuses had been removed during cardiothoracic surgical procedures and were obtained from the Second Affiliated hospital, Sun Yat-sen University (Guangzhou, China). All samples were formalin-fixed, paraffin-embedded, and pathologically diagnosed. This study was approved by the Institute Research Ethics Committee of the Cancer Center and the Second Affiliated hospital, Sun Yat-Sen University.

Two T-cell lines (Jurkat and SUP-T1) were obtained from the ATCC. Cells were cultured for less than 3 months after resuscitation and were maintained in RPMI-1640 media (Gibco Laboratories) with 10% (volume/volume) fetal bovine serum (Gibco Laboratories) at 37°C in a 5% CO_2 incubator. Cells were authenticated by short tandem repeat (STR) fingerprinting at the Medicine Lab of Forensic Medicine Department of Sun Yat-sen University (Guangzhou, China).

MicroRCURY LNA array analysis

Total RNA was extracted from five pairs of T-LBL and normal infantile thymus using the mirVana miRNA isolation kit (Ambion). Microarray chip analysis was performed and analyzed by Applied Biosystems Human MicroRNA Cards (A and B Cards, respectively; Applied Biosystems). These two panels are designed with 768 unique assays of human miRNAs (the data have been deposited in the Gene Expression Omnibus database under accession code GPL17797). Among the 768 human miRNA probes, the microarray detected 367 miRNAs in the T-LBL pairs (Supplementary Data). Before microarray analysis, RNA quality was determined using the Agilent 2100 bioanalyzer (Agilent Technologies). All the samples had an RNA integrity number greater than 7.0. The fold change was calculated by comparing the expression of miRNA in the T-LBL tumor pool and the infantile thymus in a $\log^2$ format.

RNA isolation and quantitative real-time PCR

Total RNA was isolated from formalin-fixed and paraffin-embedded tissues (FFPET) using TRIzol reagent (Invitrogen) according to the manufacturer's instructions. miRNA was extracted from all available FFPET or infant thymus tissues in which the majority of cell populations (>75%) were cells of interest (T-LBL cells in tumor biopsies and thymus cells in infant thymus tissues). A total of 2 μg RNA was reverse-transcribed using the Advantage RT-PCR kit (Clontech Laboratories, Inc.) for first-strand complementary DNA synthesis. Quantitative PCR was then carried out with primers for miR-374b, U6 snRNA, Wnt16a, Wnt16b, and AKT1 (see Supplementary Table S1) with SYBR using the ABI 7900HT fast real-time PCR system (Applied Biosystems) following a standard quantitative PCR protocol. Briefly, quantitative PCR started with the incubation of samples at 48°C for 2 minutes followed by 95°C for 15 seconds and 60°C for 1 minute. The expression level was normalized against endogenous U6 snRNA for the tested genes. The quantity of miR-374b in each T-LBL relative to the mean expression in 18 ANTs was calculated using the relative quantity (RQ) method $= 2^{-\Delta\Delta CT}$, where $\Delta\Delta C_T = (C_{T\text{miRNA}} - C_{T\text{U6RNA}})\text{T-LBL} - (C_{T\text{miRNA}} - C_{T\text{U6RNA}})\text{Mean}_{\text{ANTs}}$. Each sample was analyzed in triplicate.

Receiver operating characteristic (ROC) curve analysis was performed to determine the cutoff score for tumor "high expression" using the 0, 1 criterion (20). At the miR-374b expression RQ, the sensitivity and specificity for each outcome under study was plotted, thus generating various ROC curves. The score was selected as the cutoff value, which was closest to the point with both maximum sensitivity and specificity (21).

Plasmid construction, lentivirus production, and transduction

The pre-miR-374b precursor, anti-miR-374b (with sequence that was complementary to mature miR-374b), and the coding sequences of WNT16 and AKT1 constructs were amplified and cloned into the pCDH-CMV-MSC-EF1-coGFP cDNA expression lentivector (System Biosciences). Then, the lentiviral expression construct and packaging plasmid mix were cotransfected into 293 cells to generate recombinant lentivirus according to the manufacturer's manual. Jurkat and SUP-T1 cells were infected with recombinant lentivirus-transducing units plus 8 μg/mL Polybrene (Sigma).

MTT assay

Cell viability was measured by a 3-(4,5-dimethylthiazol-2-yl)-2, 5-diphenyl tetrazolium bromide (MTT) assay (Sigma). Briefly,

Downloaded from http://aacrjournals.org/clincancerres/article-pdf/21/21/4881/2027063/4881.pdf by guest on 24 August 2022

cells were seeded in 96-well plates and cultured. Cell viability was examined by following standard procedures. Experiments were performed in triplicate.

In vivo experiments

For *in vivo* study, 2×10^6 mixed populations of SUP-T1 cells, stably expressing miR-374b, or the vector control, were injected subcutaneously into the flanks of BALB/C-nu/nu athymic nude mice (6 mice per group). Over a 36-day period, tumor formation in nude mice was observed by measuring the tumor volume calculated by the formula $V = 0.5 \times L \times W^2$, where V, volume; L, length, and W, width. Tumors were then excised and embedded in paraffin for hematoxylin and eosin (H&E) staining and immunohistochemistry (IHC) analysis. All procedures were in accordance with the guidelines of the laboratory animal ethics committee of Sun Yat-Sen University.

Flow cytometric analysis of apoptosis

Annexin V–APC and propidium iodide (PI) stains were used to determine the percentage of cells undergoing apoptosis. Cells were cultured in RPMI-1640 media with 10% fetal bovine serum for 36 hours or treated with serum-free RPMI-1640 media for 36 hours. In the group of chemotherapy, cells were treated with indicated dose of doxorubicin for 24 hours. The apoptosis assay was conducted using the protocol supplied by the manufacturer (BioVision Inc.). Each sample was then subjected to flow cytometry analyses (Cytomics FC 500; Beckman Coulter).

Luciferase reporter assay

The putative miR-374b binding site at the 3′-UTR of WNT16 and AKT1 mRNAs was cloned downstream of the cytomegalovirus (CMV) promoter in a pMIR-REPORT vector (Ambion). Two mutant constructs were generated by either deletion or mutation.

The firefly luciferase construct was cotransfected with a control Renilla luciferase vector into Jurkat and SUP-T1 cells in the presence of either miR-374b or miR-control. A dual-luciferase assay (Promega) was performed 48 hours after transfection. The experiments were performed independently in triplicate.

Western blot analysis

Western blotting was performed according to the standard protocol with antibodies to PARP, caspase-3, cleaved caspase-3, AKT, AKT1, p-AKT, mTOR, p-mTOR, GSK3β, p-GSK3β, BAD, p-BAD, FOXO1/3, and p-FOXO1/3 (Cell Signaling Technology). Anti-Wnt16 antibody was purchased from Santa Cruz Biotechnology. GAPDH (Santa Cruz Biotechnology) was used as a normalized control. All protein bands were detected using a SuperSignal West Pico Chemiluminescent Substrate (Pierce). The lanes of Western Blotting were scanned and band densities quantified using the Quantity-One software from the Bio-Rad Image analysis systems (Bio-Rad Laboratories).

H&E staining analysis and IHC

H&E staining analysis was performed as previously described (22). IHC staining was performed on 5-μm tissue sections rehydrated through graded alcohols. Endogenous peroxidase activity was blocked with 0.3% hydrogen peroxide for 15 minutes. Antigen retrieval was performed by boiling sections in a microwave oven with 10 mmol/L citrate buffer, pH 6.0, for 15 minutes. Nonspecific binding was blocked with 10% normal rabbit serum for 10 minutes. The tissue slides were incubated with primary antibodies overnight at 4°C. Subsequently, the slides were sequentially incubated with biotinylated goat anti-rabbit immunoglobulin (IgG) at a concentration of 1:100 for 30 minutes at 37°C and then reacted with a streptavidin-peroxidase conjugate for 30 minutes at 37°C and 3′-3′ diaminobenzidine as a chromogen substrate. The nucleus was counterstained using Meyer's hematoxylin. The negative control consisted of replacing the primary antibody with normal nonspecific IgG.

Immunohistochemistry evaluation

The expression of AKT1 and Wnt16 was assessed by three independent pathologists (D. Xie, Q. Cai, and D. Qian) who were blinded to clinical follow-up data. Their conclusions were in complete agreement for 85% of cases, indicating that this scoring method was highly reproducible. If two or all three agreed with the scoring results, the value was selected. If the results were completely different, then the pathologists worked collaboratively to confirm the score.

For evaluation of AKT1 and Wnt16 IHC staining, a semiquantitative scoring criterion was used, in which both staining intensity and positive areas were recorded. A staining index (values, 0–12) obtained as the intensity of positive staining (weak, 1; moderate, 2; strong, 3) and the proportion of immune-positive cells of interest (0%, 0; <10%, 1; 10%–50%, 2; 51%–80%, 3; >80%, 4) were calculated. Finally, cases were classified into two different groups: low expression cases (score, 0–6) and cases with high expression (score, 8–12).

Statistical analysis

Statistical analysis was carried out using SPSS 16.0 (SPSS Standard version 13.0; SPSS Inc.). The Student t test was used to analyze the results expressed as mean ± SD. The χ^2 test or the Fisher exact test was used to analyze the association of miR-374b expression and clinical–pathologic parameters. The survival curves were plotted by Kaplan–Meier analysis. Differences were considered significant when the P value was less than 0.05.

Results

MiR-374b is frequently downregulated in T-LBL

To investigate the roles of miRNAs in T-LBL, miRCURY LNA array (Exiqon) containing 750 human miRNAs was performed to compare the miRNA expression profiles between T-LBL tumor samples and infantile thymus. Among the 750 human miRNA probes, the microarray detected 367 miRNAs in the T-LBL pairs. With the 2-fold cutoff point, 19 differentially expressed miRNAs (12 upregulated and seven downregulated) were detected in T-LBL tumor tissues compared with the nontumor counterparts (Supplementary Table S2). The relative expression of these miRNAs is presented as a heatmap (Fig. 1A). miR-374b, which showed lower expression in all five primary T-LBL samples than in normal infantile thymus, was chosen for further study. Quantitative PCR was performed to confirm the expression of miR-374b in 30 infantile thymus and 58 primary T-LBL samples. Consistent with the array, miR-374b was strongly downregulated in these T-LBL samples (Fig. 1B).

Downloaded from http://aacrjournals.org/clincancerres/article-pdf/21/21/4881/2027063/4881.pdf by guest on 24 August 2022

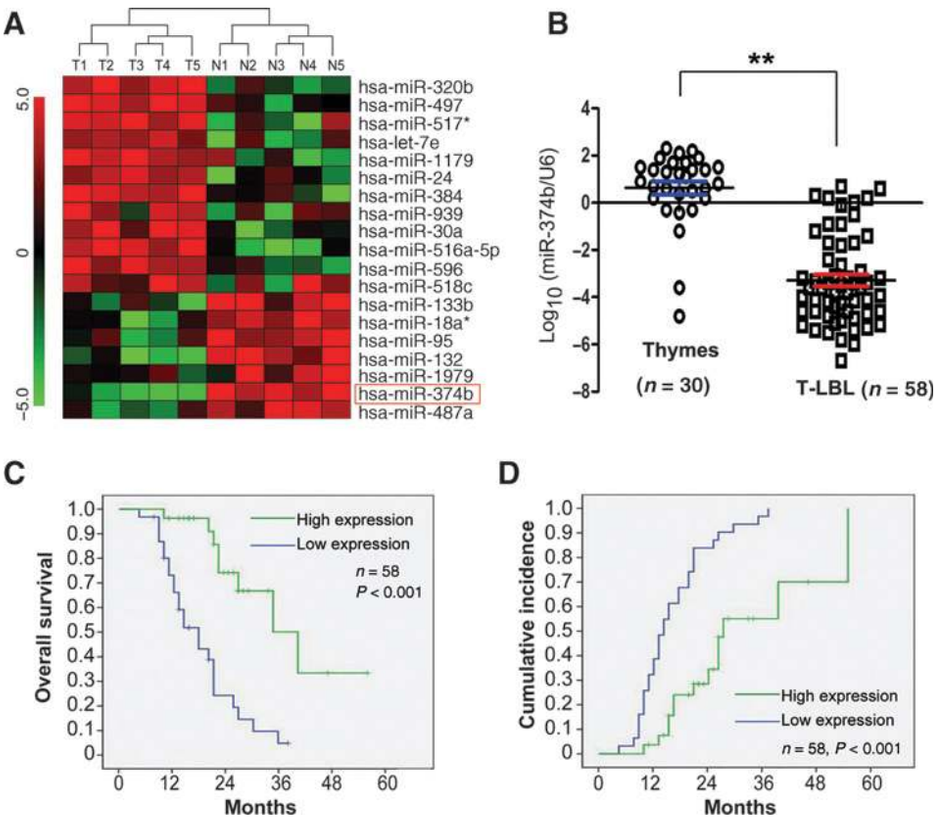

Figure 1.
Downregulation of miR-374b in T-LBL, which is associated with poor prognosis. A, hierarchical clustering heatmap of significantly differentially expressed miRNAs. B, miR-374b was significantly downregulated in 58 primary T-LBL. C, downregulation of miR-374b was significantly associated with poorer overall survival and D, higher risk of relapse. All the values represent means ± SD (**, $P < 0.01$).

Downregulation of miR-374b is associated with poor prognosis of T-LBL

To address the clinical significance of the downregulation of miR-374b in T-LBL, the correlation of miR-374b with clinical–pathologic features from these patients was studied. We first subjected the value of miR-374b expression in the 58 cases of T-LBL tissues to ROC curve analysis with respect to each clinicopathologic feature. The corresponding area under the curve and cutoff scores for high expression of miR-374b are shown in Supplementary Fig. S1 and Supplementary Table S3. In this study, ROC curve analysis for relapse in 2 years had the shortest distance from the curve to the point (i.e., 1.0, 0.0), and were used to select the cutoff value (−0.312) determined by the relapse stage of T-LBL patients. The results showed that the downregulation of miR-374b was significantly correlated with advanced clinical stage and chemotherapy resistance while no significant correlation was observed for other clinical–pathologic parameters (Supplementary Table S4). Additionally, Kaplan–Meier analysis revealed that lower miR-374b levels were associated with poorer overall survival and a higher risk of recurrence in the T-LBL cohort ($P \leq 0.05$; Fig. 1C and D). These results suggested that the downregulation of miR-374b might play an important role in the development and progression of T-LBL.

MiR-374b suppresses tumor cell growth

To explore the potential tumor-suppressive role of miR-374b in T-LBL, the miR-374b precursor was cloned and stably transfected into Jurkat and SUP-T1 cell lines. The expression of mature miR-374b was confirmed by quantitative PCR (Fig. 2A). The MTT assay showed that miR-374b inhibited cell growth compared with empty vector-transfected control cells (Fig. 2B). Furthermore, we examined the antitumor effect of miR-374b on T-LBL xenografts *in vivo*. SUP-T1-374b cells and vector control SUP-T1 cells were inoculated into female athymic nude mice. Consistent with the *in vitro* study results, miR-374b inhibited tumor formation *in vivo* (Fig. 2C). In addition, IHC staining of Ki67 was performed to detect proliferating cells. As expected, less Ki67 expression was detected in SUP-T1-374b cells than in SUP-T1-vector control cells (Fig. 2D). Moreover, loss-of-function studies revealed that depletion of miR-374b promoted cell proliferation in both Jurkat and SUP-T1 cells (Supplementary Fig. S2A and S2B). The effect of miR-374b on Jurkat xenografts was also studied. Consistent with the *in vitro* results, inhibition of miR-374b promoted tumor formation *in vivo*. In contrast, overexpression of miR-374b suppressed tumor growth in Jurkat xenografts (Supplementary Fig. 2C). These results implied that miR-374b has a strong ability to suppress tumor cell growth.

MiR-374b promotes apoptosis of T-LBL cells

To determine whether miR-374b has a proapoptotic effect on T-LBL cells, the Annexin V/PI staining cell apoptosis assay was performed. Flow cytometry analysis indicated that miR-374b dramatically promoted tumor cell apoptosis in Jurkat and SUP-T1 cells compared with the vector-transfected control cells under normal conditions ($P < 0.05$, Fig. 3A). Additionally, we examined the effect of miR-374b on serum-deprived and chemotherapy-induced apoptosis using the same cell lines. Compared with negative controls, the enhanced expression of miR-374b significantly increased the apoptotic rate of cells cultured without serum for 36 hours ($P < 0.01$, Fig. 3A), or

Downloaded from http://aacrjournals.org/clincancerres/article-pdf/21/21/4881/2027063/4881.pdf by guest on 24 August 2022

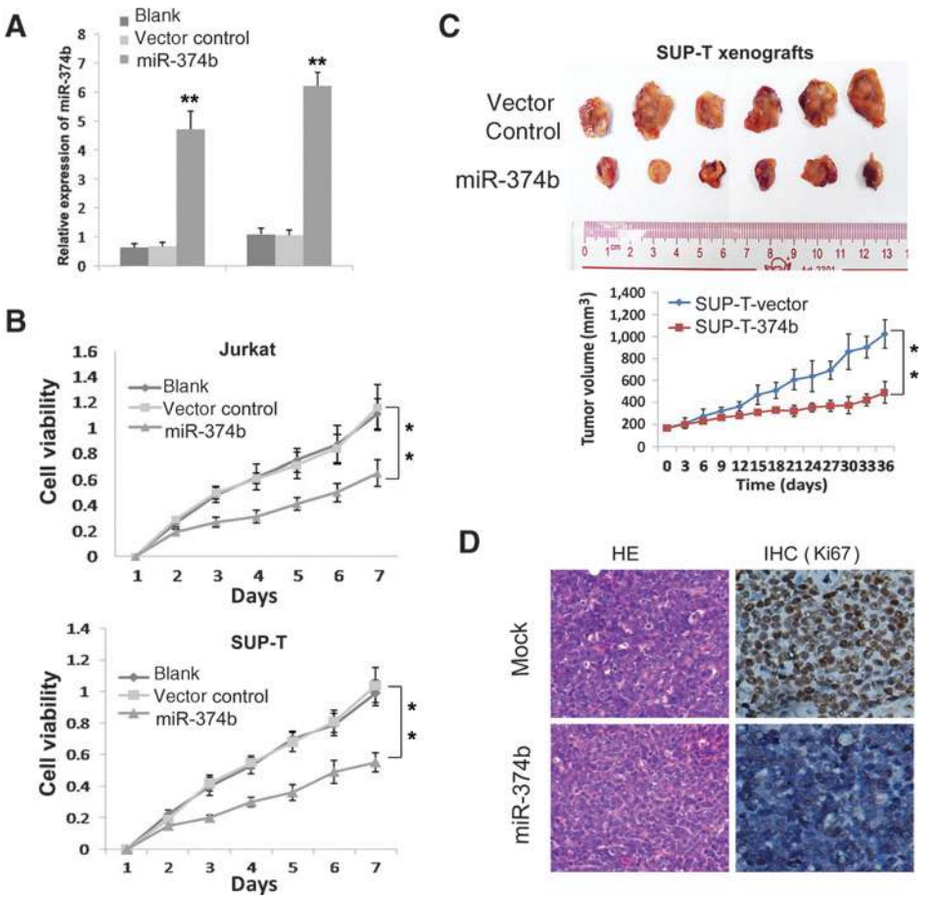

Figure 2.
miR-374b suppresses tumor cell growth *in vitro* and *in vivo*. A, relative expression of miR-374b was detected by quantitative PCR in stably transfected Jurkat (Jurkat-374b) and SUP-T1 (SUP-T1-374b) cells relative to empty vectors (Jurkat-Vector and SUP-T1-Vector). Expression was normalized against an endogenous control U6 levels. B, cell growth rate was suppressed by miR-374b in Jurkat (left) and SUP-T1 (right) cells detected by the MTT assay. Results are expressed as mean ± SD of three independent experiments (**, $P < 0.01$). C, tumor growth curves show that miR-374b inhibited tumor formation in nude mice. Tumor volume of xenografts was measured with calipers every 3 days for 36 days. The mean tumor volume in the SUP-T-374b group (457.6 ± 86.2 mm^3) was significantly smaller than that of the SUP-T-vector group (1067.9 ± 137.5 mm^3; $n = 6$, **, $P < 0.01$). D, representative images show xenograft tumors in null mice with SUP-T1-Vector and SUP-T1-374b cells. H&E staining and IHC staining of Ki67 were performed on sections of tumors excised from mice.

exposed to doxorubicin, a major drug used for chemotherapy of T-LBL, for 24 hours at the indicated concentration ($P < 0.01$, Fig. 3A). In contrast, depletion of miR-374b inhibited apoptosis in both Jurkat and SUP-T1 cells (Supplementary Fig. S2D). Moreover, Western blot analysis suggested a significant decrease in levels of pro-caspase-3, increased levels of cleaved caspase-3, and cleaved PARP in miR-374b restored cells treated with either serum deprivation or doxorubicin (Fig. 3B). Together, these results demonstrate that miR-374b promotes the apoptosis of T-LBL cells.

Wnt16 and AKT1 are direct targets of miR-374b

As miR-374b suppressed cell growth and enhanced cell apoptosis in T-LBL, we explored the molecular mechanisms responsible for the effect of miR-374b. By searching TargetScan, pictar, and miRanda, we compiled all the predicted genes for functional clustering analysis classified by DAVID 6.7, Kegg, and Panther databases (23). Based on a previously used method (24), Wnt16 and AKT1 were identified as targets of miR-374b, and which contained a putative target sequence (Fig. 4A). To validate whether Wnt16 and AKT1 were the direct downstream targets of miR-374b, fragments of the 3′-UTR of Wnt16 and AKT1 (Fig. 4A) containing the potential miR-374b binding site were cloned into a vector with the firefly luciferase reporter gene. Luciferase activity was reduced by approximately 55% and 43% compared with the control but not that of the mutant reporter (Fig. 4B). Furthermore, reverse transcription-PCR (RT-PCR) and Western blotting were used to test whether the expression of Wnt16 and AKT1 was repressed by miR-374b. The *WNT16* gene spans four exons with alternative exons 1a and 1b. Each exon 1 is associated with a unique promoter allowing the transcription of two different mRNA isoforms: Wnt16a and Wnt16b (25). However, no expression of Wnt16a was detected in either Jurkat or SUP-T1 cells using specific primers (Fig. 4C). We concluded that the isoform detected by RT-PCR and Western blotting was Wnt16b in these cell lines. Furthermore, the result showed that miR-374b downregulated the expression of Wnt16 and AKT1 at the mRNA (Fig. 4C) and protein level (Fig. 4D). Moreover, both the anti-growth and apoptosis-promoting effects of miR-374b were partly rescued when Wnt16b or AKT1 was replenished in SUP-T1-374b cells respectively (Supplementary Fig. S3A–S3C). A correlation between miR-374b levels and the expression of Wnt16 and AKT1was further examined in T-LBL tissues by IHC, and miR-374b was determined by qPCR in the same set of specimens shown in Fig. 1. miR-374b levels were inversely correlated with Wnt16 and AKT1 expression (Fig. 5A and B). Furthermore, higher Wnt16 and AKT1 levels were also associated with poorer overall survival and a higher risk of recurrence in the T-LBL cohort ($P \leq 0.05$, Fig. 5C and D), which is consistent with that of lower miR-374b levels in T-LBL specimens.

These data suggest that miR-374b may negatively regulate the expression of Wnt16 and AKT1 by directly targeting the 3′-UTR of their mRNAs.

Downloaded from http://aacrjournals.org/clincancerres/article-pdf/21/21/4881/2027063/4881.pdf by guest on 24 August 2022

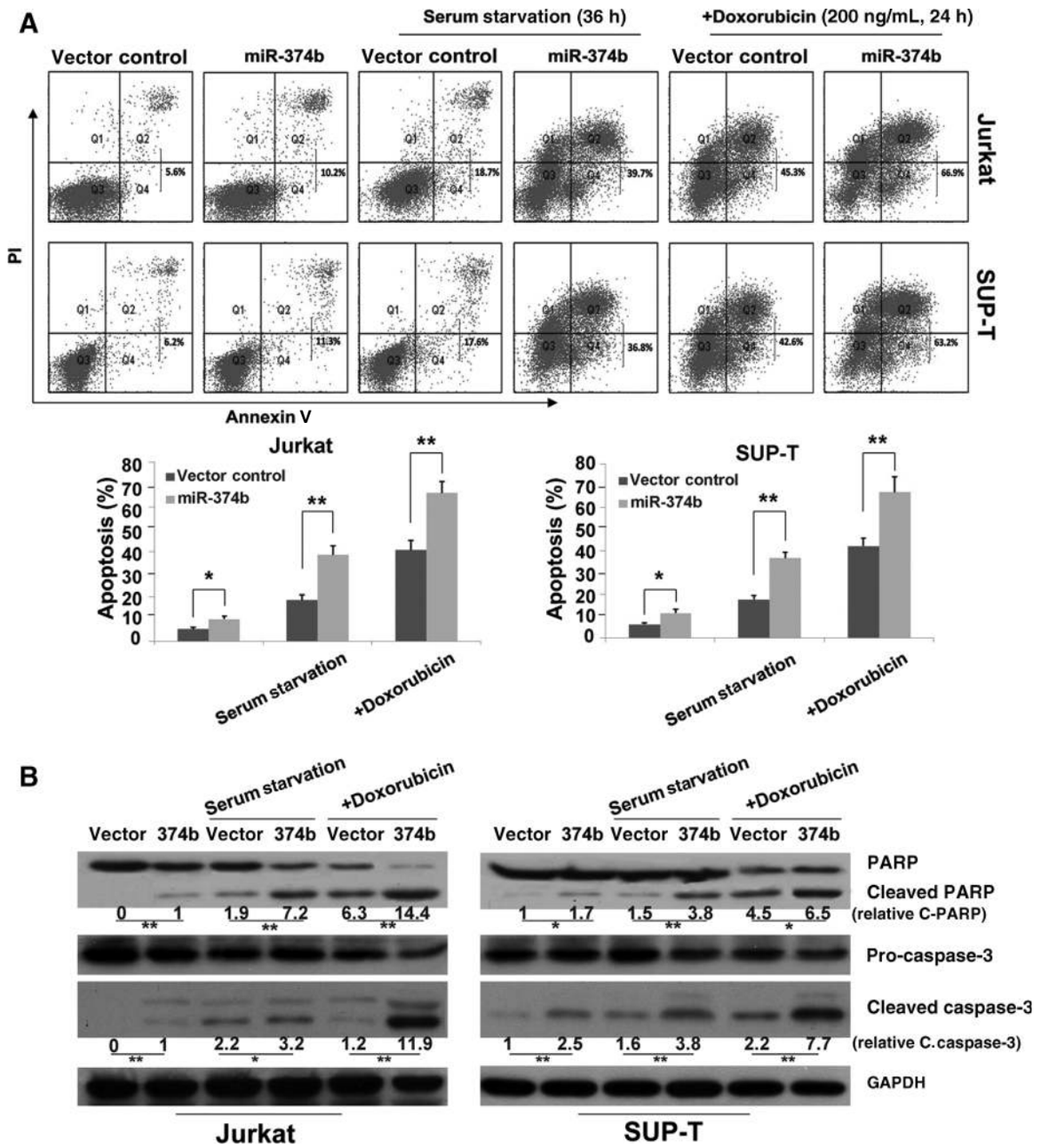

Figure 3.

miR-374b sensitizes cells to apoptosis. A, miR-374b sensitizes cells to serum starvation- or doxorubicin-induced apoptosis. Jurkat-374b, SUP-T1-374b, and vector control cells (Jurkat-Vector and SUP-T1-Vector) treated with serum-free RPMI-1640 media for 36 hours or indicated dose of doxorubicin for 24 hours. Cell apoptotic death events were monitored by Annexin V/PI staining and flow cytometry assays. The percentage of cell apoptosis was shown as the mean ± SD from three independent experiments. B, after treatment, caspase-3 and PARP levels were determined by Western blotting, and GAPDH was used as a normalized control. The quantitative values under the bands were the relative ratios of cleaved PARP, cleaved caspase-3 to GAPDH from densitometric analysis.

MiR-374b suppresses cell growth and enhances cell apoptosis through inhibiting the AKT signaling pathway

Given that both Wnt16 and AKT1 play crucial roles in the AKT signaling pathway (26, 27), the roles of miR-374b in the activation of AKT were investigated. Interestingly, the expression of phosphorylated AKT and total AKT was dramatically decreased by the restoration of miR-374b in Jurkat and SUP-T1 cells. The detection of AKT-phosphorylated substrates demonstrated levels of phosphorylated mTOR, phosphorylated BAD, and total FOXO1/3 were decreased, whereas levels of phosphorylated FOXO1/3 increased in miR-374b–overexpressing cells. However, the activation of GSK3β, another key AKT-phosphorylated substrate, was not affected by miR-374b restoration (Fig. 6A). Additionally, when we used a high dose of AKT inhibitor (40 μmol/L

Downloaded from http://aacrjournals.org/clincancerres/article-pdf/21/21/4881/2027063/4881.pdf by guest on 24 August 2022

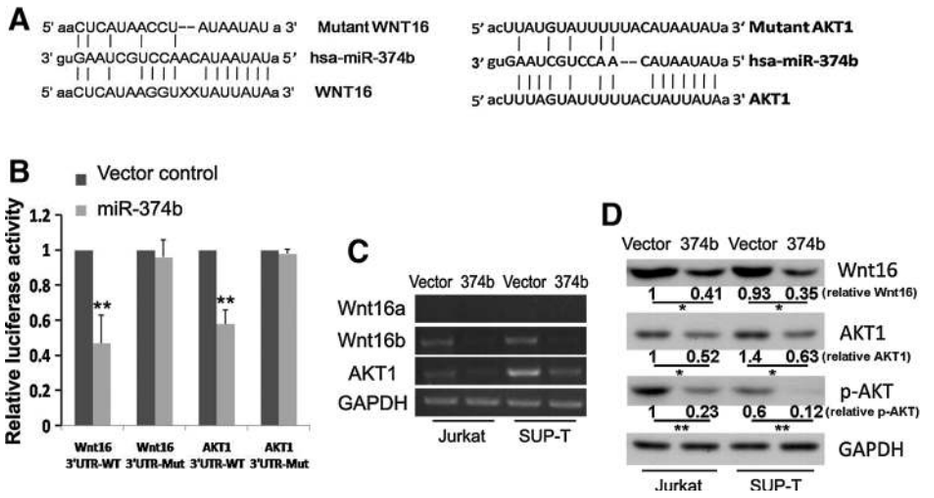

Figure 4.

AKT1 and Wnt16 are direct downstream targets of miR-374b. A, putative miR-374b-binding sequence in the 3′-UTR of AKT1 and Wnt16 mRNA. Mutations were generated in the AKT1 and Wnt16 3′-UTR sequence in the complementary site for the seed region of miR-374b as indicated. B, analysis of luciferase activity. Human AKT1 and Wnt16 3′-UTR fragment containing a wild-type or mutant miR-374b–binding sequence was cloned downstream of the luciferase reporter gene. The plasmids were transfected into empty vectors or miR-374b stably expressing cells. Renilla luciferase plasmids were cotransfected for normalization. pGL3-control vector was cotransfected as a positive control. Data of the reporter assays are the mean ± SD of three independent experiments, **, $P < 0.01$. C and D, reverse transcription-PCR (C) and Western blot analysis (D) show that miR-374b inhibits both mRNA and protein levels of AKT1 and Wnt16 in Jurkat-374b and SUP-T1-374b cells. GAPDH was used as an internal control. Only Wnt16b was detected in Jurkat and SUP-T1 cells (C). The quantitative values under the bands were the relative ratios of Wnt 16, AKT1, and p-AKT to GAPDH from densitometric analysis (D). All the values represent means ± SD (**, $P < 0.01$).

AKT inhibitor V) such that it sufficiently block AKT activation, the effect of miR-374b disappeared almost completely (Fig. 6B–D). Interestingly, the additive effect was well presented when miR-374b combined with lower dose of AKT inhibitor V (20 μmol/L; Supplementary Fig. S4). These results further confirm that miR-374b suppresses cell growth and enhances cell apoptosis through inhibiting the AKT signaling pathway.

Discussion

MiR-374b was significantly downregulated in the T-LBL tissues examined in this study, and was involved in multiple physical functions and diseases, such as lipid metabolism, renal Ca^{2+} homeostasis and vascular permeability in injury (28–31). However, little is known about the roles and mechanisms of miR-374b in the human cancer process. In the present study, we demonstrated that downregulation of miR-374b was significantly associated with a high risk of relapse and worse overall survival in T-LBL patients. Furthermore, our *in vitro* and *in vivo* studies showed that ectopic restoration of miR-374b suppressed cell proliferation and tumorigenicity and promoted cellular apoptosis by repressing Wnt-16 and AKT1 expression. Taken together, our findings emphasize the fundamental roles of miR-374b in human lymphomas, and implicate the potential application of miR-374b for prognosis prediction and therapy of T-LBL.

Cell proliferation and apoptosis play central roles in cancer development and therapy, and are regulated by multiple molecular pathways, such as Ras, P53, and AKT/PKB, among others (32–34). In the present study, we characterized AKT1 as a functional target of miR-374b. This suggested that the AKT might be a downstream signaling molecule of miR-374b and play a pivotal role. Wnt16 was another gene we identified as a target of miR-374b for the first time. The WNT pathway is a powerful signaling pathway that is widely involved in developmental processes and oncogenesis. Wnt signaling is very complicated and 19 Wnt proteins have been identified, including Wnt16 (35, 36), which has two isoforms, Wnt16a and Wnt16b. Only Wnt16b expression was detected by RT-PCR in the T-LBL cells. A similar result was observed in MRC5 human fibroblasts (26). Wnt16b was initially described as an oncogene that activated β-catenin in pre-B acute lymphoblastoid leukemia or enhanced the survival of cancer cells with or without cytotoxic therapy via a β-catenin–independent noncanonical WNT transduction pathway (37, 38). Furthermore, Binet and colleagues reported Wnt16b was identified as a new marker of senescence and over-expression of Wnt16b activated the PI3K/AKT pathway (26). Consistent with previous reports, overexpression of Wnt16b in our SUP-T1-374b cells partly rescued the levels of phospho-AKT, which was suppressed by miR-374b (Supplementary Fig. S3A). Upregulation of Wnt16b in both Jurkat and SUP-T1 blank cells enhanced the activation of AKT (Supplementary Fig. S5A). Moreover, the anti-growth and apoptosis-promoting effects of miR-374b were only slightly rescued when β-catenin was upregulated in SUP-T1-374b cells (Supplementary Fig. S5B). In addition, XAV-939, a Wnt inhibitor that augments β-catenin degradation through its stabilization of AXIN (39), at 2 μmol/L, was applied to block the Wnt/β-catenin signaling pathway in our T-LBL cells. Our results showed that there was a marked addictive effect when using XAV-939 in miR-374b-overexpression T-LBL cells (Supplementary Fig. S5C and S5D). These results further supported that inhibition of AKT activation which induced by suppressing a β-catenin-independent effect of Wnt16b may be a mechanism by which miR-374b suppresses proliferation and promotes apoptosis in T-LBL cells. Based on these findings, we hypothesized whether reintroduction of miR-374b could regulate the PI3K/AKT pathway. Our results clearly showed that phospho-AKT levels were markedly

Downloaded from http://aacrjournals.org/clincancerres/article-pdf/21/21/4881/2027063/4881.pdf by guest on 24 August 2022

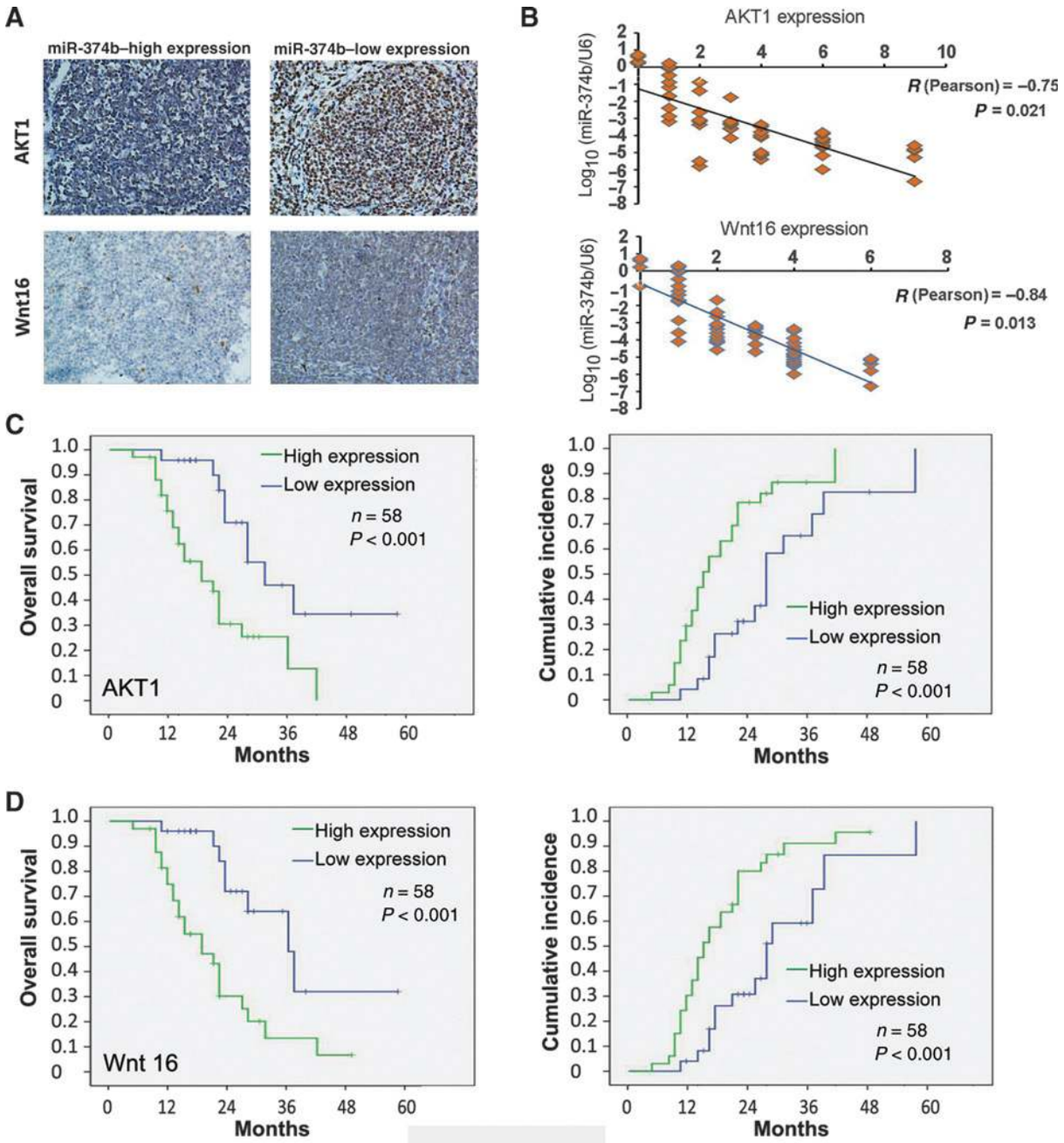

Figure 5.

The expression of AKT1 and Wnt16 was negatively correlated with the miR-374b expression level in T-LBL. A, IHC staining of AKT1 and Wnt16 in T-LBL samples. Representative images show higher expression of AKT1 and Wnt16 in samples with low miR-374b levels and lower expression of AKT1 and Wnt16 in samples with high miR-374b levels. B, negative correlation between AKT1 (left), Wnt16 (right), and miR-374b expression in 58 T-LBL samples, the correlation between miR-374b and AKT1 or Wnt16 was determined with linear regression lines and Pearson correlation significance (**, $P < 0.01$). C and D, upregulation of AKT1 (C) and Wnt16 (D) is significantly associated with poorer overall survival (left) and higher risk of relapse (right).

downregulated in miR-374b–restored T-LBL cells. To our knowledge, activated AKT promotes proliferation and decrease of apoptosis in cancer cells by phosphorylating a large number of downstream substrates containing the consensus sequence RXRXXS/T, such as mTOR, GSK3β, caspase cascade, and FoxO family members (40–42). Our results also showed that AKT/mTOR, AKT/BAD, and AKT/FoxO signaling were all inhibited followed by deregulation of phospho-AKT in the miR-374b overexpressing cells. These AKT-mediated signaling pathways play a profound role in multiple critical cellular processes, including cell proliferation and apoptosis (43, 44). These findings further support the idea that miR-374b functions

Downloaded from http://aacrjournals.org/clincancerres/article-pdf/21/21/4881/2027063/4881.pdf by guest on 24 August 2022

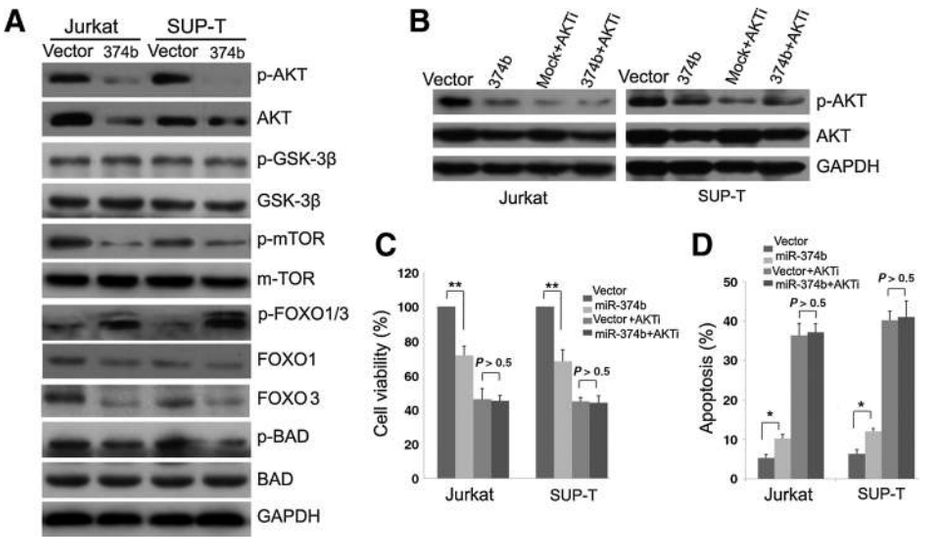

Figure 6.
MiR-374b suppresses cell growth and enhances cell apoptosis by inhibiting the AKT signaling pathway. A, Western blot analysis of the expression of AKT pathway–associated downstream factors. All data are derived from three individual experiments. B, AKT phosphorylation is significantly inhibited in cells treated with AKT inhibitor V (40 μmol/L). C and D, the anti-growth (C) and apoptosis-promoting (D) effects of miR-374b on T-LBL cells almost disappear when AKT phosphorylation is inhibited by AKT inhibitor V. Results are representative of three individual experiments. All the values represent means ± SD (**, $P < 0.01$).

mainly through the AKT signaling pathway. However, GSK3, another important AKT-phosphorylated substrate (45), was not affected by miR-374b restoration. Further studies are required to elucidate the complex interactions between miR-374b and the AKT signaling pathway. PTEN has been showed to be a tumor suppressor gene that inhibits the PI3K/AKT signaling pathway and is either deleted or mutated in high percentage of human tumors (46–48). The relationship between miR-374b and PTEN was studied subsequently. Our results showed that the expression of PTEN was not influenced by miR-374b. Depletion of PTEN enhanced the activation of AKT in both control cells and miR-374b–overexpressing cells significantly, and entirely rescued the effect of miR-374b on cell proliferation and cell apoptosis (Supplementary Fig. S6). These results suggest that miR-374b and PTEN might inhibit the AKT signaling pathway by different mechanisms.

He and colleagues reported that miR-374b was downregulated in prostate cancer tissue, and was identified as an independent predictor of biochemical recurrence-free survival (31). Our result also clearly showed that miR-374b was frequently downregulated in T-LBL tissues. However, a most recently study showed that the expression levels of miR-374b was not different between HCC and noncancerous liver tissues (49), suggesting that the functions of miR-374b in tumorigenesis are complicated and may be tumor-type-specific. In the cohorts of our T-LBL patients, low expression of miR-374b was found to correlate positively with a high risk of relapse in T-LBL patients, and miR-374b downregulation was a strong and independent predictor for poor survival. In our clinical T-LBL tissues, we found that the expression levels of both AKT1 and Wnt16 were inversely correlated with miR-374b levels. Therefore, miR-374b might be a promising biomarker for predicting relapse and survival of T-LBL patients. Collectively, these results suggest that the functional loss of miR-374b might result in the enhanced expression of AKT1 and Wnt16, and in turn, the promotion of cellular proliferation and the resistance of cells to serum deprivation/anthracycline-induced apoptosis at least in part, which consequently favors tumor progression. Thus, this study suggests the examination of miR-374b expression and its downstream functional targets could be used as an effective additional tool to predict the relapse and outcome of T-LBL patients and to optimize clinical decisions. Clearly, further studies are required to clarify the mechanisms of miR-374b regulation of cell survival and apoptosis.

In summary, this report describes an altered miRNA expression pattern in T-LBL and demonstrates the potential role of miR-374b in tumorigenesis. Furthermore, functional studies of miR-374b suggested a critical role for miR-374b in cell proliferation and apoptosis by regulating the AKT signaling pathway. Moreover, our results provide a basis for the concept that low expression of miR-374b may be a novel predictor of disease relapse and an independent prognostic factor for T-LBL patients, enabling clinicians to identify high-risk patients that require treatment that is more intensive. Thus, targeting the miR-374b pathway may represent a new therapeutic strategy to improve the therapy and survival of patients with T-LBL or other cancers.

Disclosure of Potential Conflicts of Interest

No potential conflicts of interest were disclosed.

Authors' Contributions

Conception and design: Q. Cai, D. Qian, D. Xie
Development of methodology: Q. Cai, D. Qian, H. Deng
Acquisition of data (provided animals, acquired and managed patients, provided facilities, etc.): Q. Cai, D. Qian, K. Chen, H. Deng, H. Huang, X. Sun, S. Lu
Analysis and interpretation of data (e.g., statistical analysis, biostatistics, computational analysis): Q. Cai, D. Qian, K. Chen, D. Xie
Writing, review, and/or revision of the manuscript: Q. Cai, D. Qian, K. Chen, D. Xie
Administrative, technical, or material support (i.e., reporting or organizing data, constructing databases): Q. Cai, D. Qian, K. Chen, H. Deng, H. Rao, Y. Liao
Study supervision: Q. Cai, H. Rao, Z. Yuan

Acknowledgments

The authors thank Prof. Ruihua Xu (Cancer Center, Sun Yat-sen University, Guangzhou, P.R. China) and Prof. Ping Wang (Tianjin Medical University Cancer Institute and Hospital, Tianjin, P.R. China) for their critical review of the article.

Downloaded from http://aacrjournals.org/clincancerres/article-pdf/21/21/4881/2027063/4881.pdf by guest on 24 August 2022

Grant Support

The work was supported by the National Natural Science Foundation of China (NO.81372883, NO.81001052, NO.81225018, NO.81401948), the Science and Technology Planning Project of Guangdong Province, China (2011B031800222), the Young Talents Project of Sun Yat-sen University Cancer Center (to Q. Cai), the Young Talents Project of Sun Yat-sen University (to Q. Cai), and the Natural Science Foundation of Guangdong Province, China (8151008901000043). The work was also supported by the Sister Institution Network Fund of the MD Anderson Cancer Center (to H. Rao).

The costs of publication of this article were defrayed in part by the payment of page charges. This article must therefore be hereby marked *advertisement* in accordance with 18 U.S.C. Section 1734 solely to indicate this fact.

Received December 25, 2014; revised May 11, 2015; accepted June 4, 2015; published OnlineFirst June 22, 2015.

References

1. Bartel DP. MicroRNAs: genomics, biogenesis, mechanism, and function. Cell 2004;116:281–97.
2. He L, Hannon GJ. MicroRNAs: small RNAs with a big role in gene regulation. Nat Rev Genet 2004;5:522–31.
3. Calin GA, Croce CM. MicroRNA signatures in human cancers. Nat Rev Cancer 2006;6:857–66.
4. Fabbri M, Croce CM. Role of microRNAs in lymphoid biology and disease. Curr Opin Hematol 2011;18:266–72.
5. Jones K, Nourse JP, Keane C, Bhatnagar A, Gandhi MK. Plasma microRNA are disease response biomarkers in classical Hodgkin lymphoma. Clin Cancer Res 2014;20:253–64.
6. A clinical evaluation of the International Lymphoma Study Group classification of non-Hodgkin's lymphoma. The Non-Hodgkin's Lymphoma Classification Project. Blood 1997;89:3909–18.
7. Portell CA, Sweetenham JW. Adult lymphoblastic lymphoma. Cancer J 2012;18:432–8.
8. Groves FD, Linet MS, Travis LB, Devesa SS. Cancer surveillance series: non-Hodgkin's lymphoma incidence by histologic subtype in the United States from 1978 through 1995. J Natl Cancer Inst 2000;92:1240–51.
9. Rosen PJ, Feinstein DI, Pattengale PK, Tindle BH, Williams AH, Cain MJ, et al. Convoluted lymphocytic lymphoma in adults: a clinicopathologic entity. Ann Intern Med 1978;89:319–24.
10. Bouabdallah R, Xerri L, Bardou VJ, Stoppa AM, Blaise D, Sainty D, et al. Role of induction chemotherapy and bone marrow transplantation in adult lymphoblastic lymphoma: a report on 62 patients from a single center. Ann Oncol 1998;9:619–25.
11. Morel P, Lepage E, Brice P, Dupriez B, D'Agay MF, Fenaux P, et al. Prognosis and treatment of lymphoblastic lymphoma in adults: a report on 80 patients. J Clin Oncol 1992;10:1078–85.
12. Le Gouill S, Lepretre S, Briere J, Morel P, Bouabdallah R, Raffoux E, et al. Adult lymphoblastic lymphoma: a retrospective analysis of 92 patients under 61 years included in the LNH87/93 trials. Leukemia 2003;17:2220–4.
13. Hoelzer D, Gokbuget N, Digel W, Faak T, Kneba M, Reutzel R, et al. Outcome of adult patients with T-lymphoblastic lymphoma treated according to protocols for acute lymphoblastic leukemia. Blood 2002;99:4379–85.
14. Croce CM. MicroRNAs and lymphomas. Ann Oncol 2008;19 Suppl 4:iv39–40.
15. Eis PS, Tam W, Sun L, Chadburn A, Li Z, Gomez MF, et al. Accumulation of miR-155 and BIC RNA in human B cell lymphomas. Proc Natl Acad Sci U S A 2005;102:3627–32.
16. Lawrie CH, Soneji S, Marafioti T, Cooper CD, Palazzo S, Paterson JC, et al. MicroRNA expression distinguishes between germinal center B cell-like and activated B cell-like subtypes of diffuse large B cell lymphoma. Int J Cancer 2007;121:1156–61.
17. Medina PP, Nolde M, Slack FJ. OncomiR addiction in an *in vivo* model of microRNA-21-induced pre-B-cell lymphoma. Nature 2010;467:86–90.
18. Akao Y, Nakagawa Y, Kitade Y, Kinoshita T, Naoe T. Downregulation of microRNAs-143 and -145 in B-cell malignancies. Cancer Sci 2007;98:1914–20.
19. Mussolin L, Holmes AB, Romualdi C, Sales G, D'Amore ES, Ghisi M, et al. An aberrant microRNA signature in childhood T-cell lymphoblastic lymphoma affecting CDKN1B expression, NOTCH1 and growth factor signaling pathways. Leukemia 2014;28:1909–12.
20. Remmele W, Stegner HE. [Recommendation for uniform definition of an immunoreactive score (IRS) for immunohistochemical estrogen receptor detection (ER-ICA) in breast cancer tissue]. Pathologe 1987;8:138–40.
21. Zhang JX, Qian D, Wang FW, Liao DZ, Wei JH, Tong ZT, et al. MicroRNA-29c enhances the sensitivities of human nasopharyngeal carcinoma to cisplatin-based chemotherapy and radiotherapy. Cancer Lett 2013;329:91–8.
22. Qian D, Zhang B, He LR, Cai MY, Mai SJ, Liao YJ, et al. The telomere/telomerase binding factor PinX1 is a new target to improve the radiotherapy effect of oesophageal squamous cell carcinomas. J Pathol 2013;229:765–74.
23. Huang da W, Sherman BT, Lempicki RA. Systematic and integrative analysis of large gene lists using DAVID bioinformatics resources. Nat Protoc 2009;4:44–57.
24. Lagana A, Forte S, Russo F, Giugno R, Pulvirenti A, Ferro A. Prediction of human targets for viral-encoded microRNAs by thermodynamics and empirical constraints. J RNAi Gene Silencing 2010;6:379–85.
25. Fear MW, Kelsell DP, Spurr NK, Barnes MR. Wnt-16a, a novel Wnt-16 isoform, which shows differential expression in adult human tissues. Biochem Biophys Res Commun 2000;278:814–20.
26. Binet R, Ythier D, Robles AI, Collado M, Larrieu D, Fonti C, et al. WNT16B is a new marker of cellular senescence that regulates p53 activity and the phosphoinositide 3-kinase/AKT pathway. Cancer Res 2009;69:9183–91.
27. Green BD, Jabbour AM, Sandow JJ, Riffkin CD, Masouras D, Daunt CP, et al. Akt1 is the principal Akt isoform regulating apoptosis in limiting cytokine concentrations. Cell Death Differ 2013;20:1341–9.
28. Pan S, Zheng Y, Zhao R, Yang X. MicroRNA-130b and microRNA-374b mediate the effect of maternal dietary protein on offspring lipid metabolism in Meishan pigs. Br J Nutr 2013;109:1731–8.
29. Gong Y, Renigunta V, Himmerkus N, Zhang J, Renigunta A, Bleich M, et al. Claudin-14 regulates renal Ca(+)(+) transport in response to CaSR signalling via a novel microRNA pathway. EMBO J 2012;31:1999–2012.
30. Pan S, Zheng Y, Zhao R, Yang X. miRNA-374 regulates dexamethasone-induced differentiation of primary cultures of porcine adipocytes. Horm Metab Res 2013;45:518–25.
31. He HC, Han ZD, Dai QS, Ling XH, Fu X, Lin ZY, et al. Global analysis of the differentially expressed miRNAs of prostate cancer in Chinese patients. BMC Genomics 2013;14:757.
32. Steelman LS, Franklin RA, Abrams SL, Chappell W, Kempf CR, Basecke J, et al. Roles of the Ras/Raf/MEK/ERK pathway in leukemia therapy. Leukemia 2011;25:1080–94.
33. Molchadsky A, Rivlin N, Brosh R, Rotter V, Sarig R. p53 is balancing development, differentiation and de-differentiation to assure cancer prevention. Carcinogenesis 2010;31:1501–8.
34. Nogueira V, Park Y, Chen CC, Xu PZ, Chen ML, Tonic I, et al. Akt determines replicative senescence and oxidative or oncogenic premature senescence and sensitizes cells to oxidative apoptosis. Cancer Cell 2008;14:458–70.
35. Anastas JN, Moon RT. WNT signalling pathways as therapeutic targets in cancer. Nat Rev Cancer 2013;13:11–26.
36. Sun Y, Campisi J, Higano C, Beer TM, Porter P, Coleman I, et al. Treatment-induced damage to the tumor microenvironment promotes prostate cancer therapy resistance through WNT16B. Nat Med 2012;18:1359–68.
37. Johnson LM, Price DK, Figg WD. Treatment-induced secretion of WNT16B promotes tumor growth and acquired resistance to chemotherapy: implications for potential use of inhibitors in cancer treatment. Cancer Biol Ther 2013;14:90–1.
38. Mazieres J, You L, He B, Xu Z, Lee AY, Mikami I, et al. Inhibition of Wnt16 in human acute lymphoblastoid leukemia cells containing the t(1;19) translocation induces apoptosis. Oncogene 2005;24:5396–400.
39. Huang SM, Mishina YM, Liu S, Cheung A, Stegmeier F, Michaud GA, et al. Tankyrase inhibition stabilizes axin and antagonizes Wnt signalling. Nature 2009;461:614–20.

Downloaded from http://aacrjournals.org/clincancerres/article-pdf/21/21/4881/2027063/4881.pdf by guest on 24 August 2022

40. Vivanco I, Sawyers CL. The phosphatidylinositol 3-Kinase AKT pathway in human cancer. Nat Rev Cancer 2002;2:489–501.
41. Testa JR, Bellacosa A. AKT plays a central role in tumorigenesis. Proc Natl Acad Sci U S A 2001;98:10983–5.
42. Osaki M, Oshimura M, Ito H. PI3K-Akt pathway: its functions and alterations in human cancer. Apoptosis 2004;9:667–76.
43. Engelman JA. Targeting PI3K signalling in cancer: opportunities, challenges and limitations. Nat Rev Cancer 2009;9:550–62.
44. Slomovitz BM, Coleman RL. The PI3K/AKT/mTOR pathway as a therapeutic target in endometrial cancer. Clin Cancer Res 2012;18:5856–64.
45. Zoncu R, Efeyan A, Sabatini DM. mTOR: from growth signal integration to cancer, diabetes and ageing. Nat Rev Mol Cell Biol 2011;12:21–35.
46. Mullighan CG, Goorha S, Radtke I, Miller CB, Coustan-Smith E, Dalton JD, et al. Genome-wide analysis of genetic alterations in acute lymphoblastic leukaemia. Nature 2007;446:758–64.
47. Silva A, Yunes JA, Cardoso BA, Martins LR, Jotta PY, Abecasis M, et al. PTEN posttranslational inactivation and hyperactivation of the PI3K/Akt pathway sustain primary T cell leukemia viability. J Clin Invest 2008;118:3762–74.
48. Chow LM, Baker SJ. PTEN function in normal and neoplastic growth. Cancer Lett 2006;241:184–96.
49. Zhao Q, Li T, Qi J, Liu J, Qin C. The miR-545/374a cluster encoded in the Ftx lncRNA is overexpressed in HBV-related hepatocellular carcinoma and promotes tumorigenesis and tumor progression. PLoS ONE 2014;9:e109782.

Downloaded from http://aacrjournals.org/clincancerres/article-pdf/21/21/4881/2027063/4881.pdf by guest on 24 August 2022